Human Molecular Genetics, 2006, Vol. 15, No. 9 ***1413–1422***
doi:10.1093/hmg/ddl064
Advance Access published on March 16, 2006

Mutations in *SOX2* cause anophthalmia-esophageal-genital (AEG) syndrome

Kathleen A. Williamson[1], Ann M. Hever[1], Joe Rainger[1], R. Curtis Rogers[4], Alex Magee[2], Zdenek Fiedler[3], Wee Teik Keng[1], Freddie H. Sharkey[1], Niolette McGill[1], Clare J. Hill[5], Adele Schneider[6], Mario Messina[7], Peter D. Turnpenny[8], Judy A. Fantes[1], Veronica van Heyningen[1] and David R. FitzPatrick[1,*]

[1]Medical Genetics Section, MRC Human Genetics Unit, Western General Hospital, Edinburgh EH4 2XU, UK, [2]Regional Genetics Service A Floor, Belfast City Hospital, Lisburn Road, Belfast BT9 7AB, UK, [3]Department of Biological and Biochemical Sciences, University Pardubice, Czech Republic, [4]Greenwood Genetic Center, 1 Gregor Mendel Circle, Greenwood, South Carolina 29646, USA, [5]Institute of Medical Genetics, University Hospital of Wales, Cardiff CF14 4XW, UK, [6]Department of Clinical Genetics, Albert Einstein Medical Center, Philadelphia, PA, USA, [7]Section of Pediatric Surgery, Department of Pediatrics, Obstetrics and Reproductive Medicine, University of Siena, Italy and [8]Institute of Biomedical and Clinical Science, Peninsula Medical School, Exeter, UK

Received December 23, 2005; Revised and Accepted March 10, 2006

We report heterozygous, loss-of-function *SOX2* mutations in three unrelated individuals with Anophthalmia-Esophageal-Genital (AEG) syndrome. One previously reported case [Rogers, R.C. (1988) Unknown cases. Proceedings of the Greenwood Genetic Center. 7, 57.] has a 2.7 Mb deletion encompassing *SOX2* and associated with a cryptic translocation t(3;7)(q28;p21.3). The deletion and translocation breakpoints on chromosome 3q are >8.6 Mb apart and both chromosome rearrangements have occurred *de novo*. Another published case [Petrackova *et al.* (2004) Association of oesophageal atresia, anophthalmia and renal duplex. *Eur. J. Pediatr.*, 163, 333–334.] has a *de novo* nonsense mutation, Q55X. A previously unreported case with severe bilateral microphthalmia and oesophageal atresia has a *de novo* missense mutation, R74P, that alters a highly evolutionarily conserved residue within the high mobility group domain, which is critical for DNA-binding of SOX2. In a yeast one-hybrid assay, this mutation abolishes Sox2-induced activation of the chick delta-crystallin DC5 enhancer. Four other reported AEG syndrome cases were extensively screened and do not have detectable *SOX2* mutations. Two of these cases have unilateral eye malformations. *SOX2* mutations are known to cause severe bilateral eye malformations but this is the first report implicating loss of function mutations in this transcription factor in oesophageal malformations. *SOX2* is expressed in the developing foregut in mouse and zebrafish embryos and an apparently normal pattern of expression is maintained in *Shh*−/− mouse embryos, suggesting either that Sox2 acts upstream of Shh or functions in a different pathway. Three-dimensional reconstructions of the major morphological events in the developing foregut and eye from Carnegie Stages 12 and 13 human embryos are presented and compared with the data from model organisms. SOX2, with NMYC and CHD7, is now the third transcriptional regulator known to be critical for normal oesophageal development in humans.

INTRODUCTION

Anophthalmia-Esophageal-Genital (AEG) syndrome (OMIM 600992) is an association of anophthalmia/microphthalmia, oesophageal atresia with or without tracheo-oesophageal fistula, and urogenital anomalies—most commonly cryptorchidism, hypospadias and micropenis. This association, first described specifically by Rogers (1) and named by Shah *et al*. (2), is reported in 20 cases (1–15). In 15 of these cases the eye phenotype is bilateral: 12 anophthalmia, 1

*To whom correspondence should be addressed. Tel: +44 1313322471; Fax: +44 1314678456; Email: david.fitzpatrick@hgu.mrc.ac.uk

microphthalmia and 2 microphthalmia with a different phenotype contralaterally.

Normal dosage of the *SOX2* gene is critical for human eye development. *SOX2* mutations have been reported in 12 cases of anophthalmia/microphthalmia to date. These mutations are heterozygous and include deletion of the whole gene (16,17) and intragenic deleterious point mutations (16,18–20). The eye phenotypes associated with *SOX2* mutation are mostly bilateral and severe, with 15–25% of cases with these phenotypes showing mutation of this gene. Extra-ocular abnormalities are common, particularly neurocognitive impairments and seizures. Urogenital anomalies are reported in males with *SOX2* anophthalmia syndrome, most commonly cryptorchidism, hypospadias and micropenis (16,19).

SOX2 is a high mobility group (HMG) domain class of transcriptional regulator (21). The HMG domain is highly conserved among SOX proteins and is critical for correct binding to interacting proteins and to target DNA sequences (22,23). In mouse, *Sox2* expression is first detected in the pre-implantation embryo, predominates in the developing central nervous system and is present during early eye development in head surface ectoderm and the derived lens placode (24,25). In chicken and zebrafish, *Sox2* is expressed during all stages of eye development: in the optic vesicle, head surface ectoderm and derived lens placode (chicken) or eye field (zebrafish) through to the neural retina (24,26). Additional sites of *Sox2* expression include the prospective neural plate, peripheral nervous system, nasal and otic placodes, bronchii and the germ cells of both sexes (25–29). *Sox2* expression has also been demonstrated in the early endoderm of the presumptive oesophagus and continues throughout the development of the rostral region of the gut in chick embryos, where high levels of expression are maintained specifically in the oesophageal epithelium (27,29). In the adult mouse, Sox2 protein persists in regions of the brain, including the cortex, thalamus, hippocampus and corpus callosum (30), and in oocytes (25). Homozygous $Sox2^{\beta}$ null mouse embryos die in the pre-implantation period, heterozyotes are viable with reduced male fertility as the only known abnormality (25).

We report *SOX2* mutation in three cases of AEG syndrome. We use three-dimensional reconstruction of human embryos to show the morphological events involved in the separation of the trachea and oesophagus and demonstrate Sox2 protein expression in the developing oesophagus in mouse and zebrafish embryos.

RESULTS

FISH analysis

Fluorescence *in situ* hybridization (FISH) analysis of metaphase chromosomes showed that a BAC clone containing *SOX2*, RP11-43F17, was deleted in Case 1 (Fig. 1A). Neither parent was deleted for RP11-43F17. Subsequent FISH analysis established the size of the deletion as 2.7 Mb, extending from RP11-145M9 (AC007620) to RP11-296J4 (AC109131) in 3q26.33. A submicroscopic translocation involving the deleted chromosome 3 was also identified by FISH analysis; BAC clone RP11-332P22 (AC092952) spans the 3q28 breakpoint and RP11-135E21 (12468571-12583311) spans the 7p21.3 breakpoint. Metaphase chromosome preparations or interphase nuclei were not available for Cases 5, 6 and 7. In Case 4, RP11-43F17 was used for interphase FISH analysis of nuclei isolated from snap-frozen spleen. Two clear locus-specific signals were seen in at least five good quality interphase nuclei, thus excluding large-scale deletions within the *SOX2* locus (data not shown).

Point mutation analysis

Seven AEG syndrome patients were studied for point mutations in *SOX2*. DHPLC analysis of overlapping PCR fragments covering the entire *SOX2* coding and untranslated regions revealed no pattern differences in Cases 1, 4, 5, 6 and 7. Clear pattern differences were observed for the coding region in Cases 2 and 3. Direct sequencing of independent PCR fragments from blood DNA in Cases 2 and 3 revealed heterozygosity. Case 2 carries the transition c.163C>T, causing the nonsense mutation Q55X. (Fig. 1B). This mutation is novel and was not found in each parent (Fig. 1B). The mutation is predicted to result in the production of protein truncated within the HMG domain and therefore with no DNA-binding or transactivation activity (*SOX2* is a single exon gene and nonsense-mediated decay is not predicted to occur).

Case 3 carries the transversion c.221G>C, causing the missense mutation R74P (Fig. 1C). Again, this mutation is novel and was not found in each parent (Fig. 1C). The R74 residue is within the HMG domain and is invariant in all known *SOX2*/*Sox2* genes and is conserved in all human *SOX* group B genes. Substitution of R74 by proline is predicted to disrupt the structure of the HMG domain and severely compromise its DNA-binding and transactivation activity. Compatible with this prediction are the results of the yeast one hybrid analysis. In this assay system, wild-type (WT) chick *Sox2* co-transfected with WT chick *Pax6* activate the *His3* gene cloned downstream of the chick delta crystallin DC5 enhancer (Fig. 2A). Using R72P, the chick equivalent of the human R74P missense mutation, activation by mutant Sox2 is lost (Fig. 2B). Indeed, this mutation can partially antagonize the activation by WT *Sox2* (Fig. 2C).

Human embryo analysis

The foregut and eye domains of five normal human embryos at Carnegie Stage 12 and 13 were examined as three-dimensional digital reconstructions following optical projection tomography (OPT). Representative embryos were selected for domain painting and three-dimensional visualization (Fig. 3). This demonstrated that initiation of the lung bud outgrowth from the ventral foregut is coincident with optic vesicle outgrowth from the forebrain at CS12 (Fig. 3A and B). By CS13 the trachea and bronchi are well-defined structures and lens pits are clearly visible (Fig. 3B). Digital sectioning of the point of separation between the foregut and lung bud at CS12 revealed a keyhole-shaped lumen (Fig. 4A and B) just above the point of separation (Fig. 4C and D). At the point of fusion there was marked ventral thickening of endoderm around the lung bud. Just below the point of fusion (Fig. 4E and F), the dorsal oesophagus and ventral lung bud have

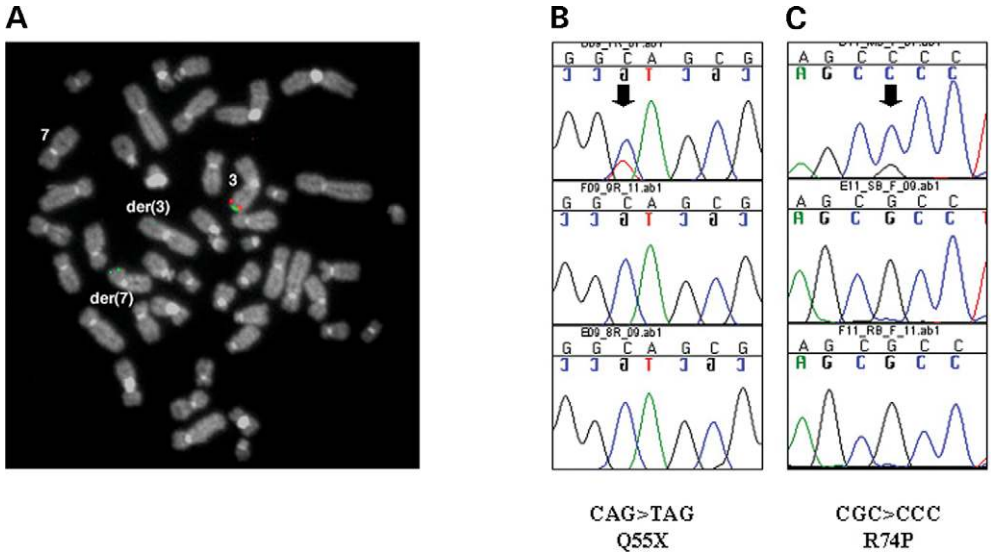

Figure 1. *SOX2* mutations in AEG syndrome. (**A**) A translocation-associated whole gene deletion is detected in Case 1. Metaphase chromosomes were hybridized with BAC clone RP11-43F17 (red signal) and chr3q telomere clone GSI-56H22 (green signal). Both red and green signals are present on the normal chr3, but the second green telomere signal has been translocated to the p telomere of the der(7). There is no red signal on either the der(3) or the der(7) chromosomes showing that one copy of the *SOX2* clone, RP11-43F17, is deleted. (**B** and **C**) Heterozygous point mutations are detected in Case 2 (B) and Case 3 (C). For each electropherogram panel the top sequence trace is from the affected Case, the middle from the unaffected mother and the bottom from the unaffected father. Case 2 has the *de novo* transition c.163C>T causing the nonsense mutation Q55X. Case 3 has the *de novo* transversion c.221G>C causing the missense mutation R74P.

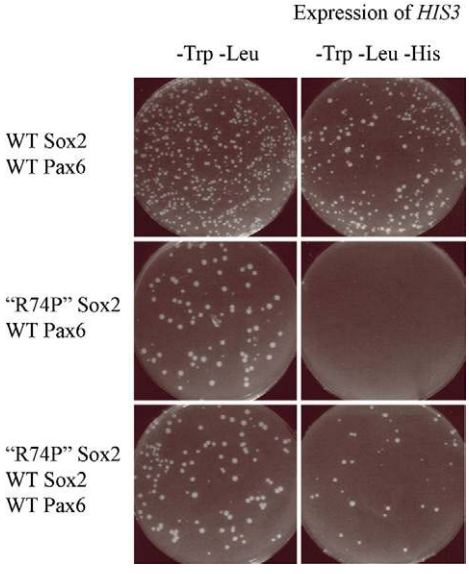

Figure 2. Functional analysis of HMG missense mutation in yeast one hybrid system. The missense mutation R72P was created in chick Sox2. This is equivalent to the human R74P missense mutation and is represented in the figure as 'R74P'. To assess the transactivation activity of this mutation a yeast one hybrid system was used. Top panels: WT Sox2 and Pax6 chick expression constructs grow in both the presence (left hand panel) or absence (right hand panel) of histidine indicating their ability to transactivate the *His3* gene by binding to the upstream delta-crystallin DC5 enhancer element. Middle panels: substitution of WT Sox2 for mutant 'R74P' Sox2 prevents growth in the absence of histidine (right hand panel), indicating that normal co-operation with Pax6 and transactivation from the DC5 enhancer element is abolished. Bottom panels: re-introduction of WT Sox2 in the presence of mutant 'R74P' Sox2 shows a reduced number of colonies in the absence of histidine (right hand panel) when compared with WT Sox2 alone, indicating partial antagonism of the mutant protein for transactivation from the DC5 enhancer element.

a 'figure of eight' configuration. At CS13, the position of separation between the trachea and oesophagus, along the long axis of the embryo and the shape of the lumen (Fig. 4F) is very similar to that seen at CS12 in spite of marked differences in the caudal structures (Fig. 3B). However, at CS13 there was no evidence of ventral thickening surrounding the lumen at the point of separation (data not shown).

Immunohistochemistry

Site- and stage-specific developmental expression of *Sox2* has been well documented in many embryonic tissues. The role of *Sox2* in foregut development has been excellently documented in chick embryos but not in other species. Here, we demonstrate strong, specific expression of Sox2 in the oesophagus, trachea, and main bronchii of mouse embryos at 11.5 gestational days (GD) (Fig. 5A and B) and 14.5 GD (Fig. 5C and D). This expression pattern was maintained in *Shh*−/− embryos at 11.5 GD (Fig. 5E and F) in spite of an apparent tracheo-oesophageal malformation in one of the embryos (Fig. 5E). There is a suggestion that the immunostaining of Sox2 is reduced in the *Shh*−/− embryos when compared with WT, but this has not been rigourously assessed using a fully quantitative method. The oesophageal expression of Sox2 is highly evolutionarily conserved and can be clearly seen in 5-day-old zebrafish embryos (Fig. 6A and B).

DISCUSSION

SOX genes are defined as encoding a HMG1 DNA-binding domain with >60% sequence homology to the HMG

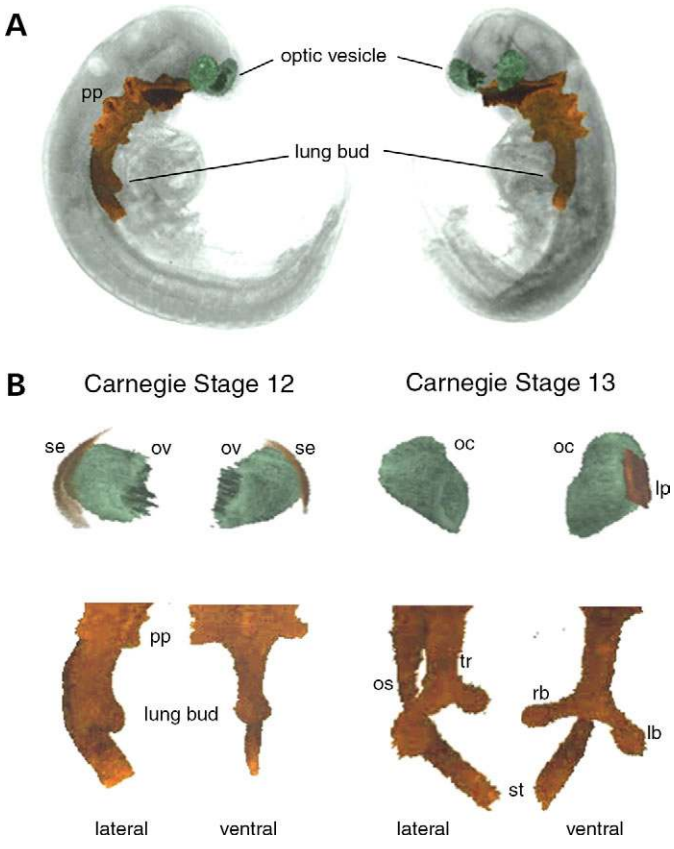

Figure 3. Three-dimensional reconstruction of eye and foregut development in early human embryos. (**A**) This panel shows two opposite lateral views of the same human embryo at CS12. The optic vesicles have been rendered in green following definition on two-dimensional digital sections of OPT reconstruction using the MAPaint program. The foregut from the pharyngeal pouches (pp) to just caudal to the lung bud is painted in red. (**B**) The panel below the Carnegie Stage 12 legend shows the isolated painted domains from the embryo in (A). The top pair of images are the optic vesicles (ov) in green with the suface ectoderm (se) in red. The lower paired images are lateral and ventral views of the foregut showing the early lung bud and prominent pharyngeal pouches (pp). The panel below the Carnegie Stage 13 legend shows the isolated painted domains from CS13 human embryos. The top pair of images are the optic cup (oc) in green with the lens pit (lp) in red. The lower paired images are lateral and ventral views of the clearly defined trachea (tr) with left (lb) and right (rb) main bronchi positioned ventral to the oesophagus (os).

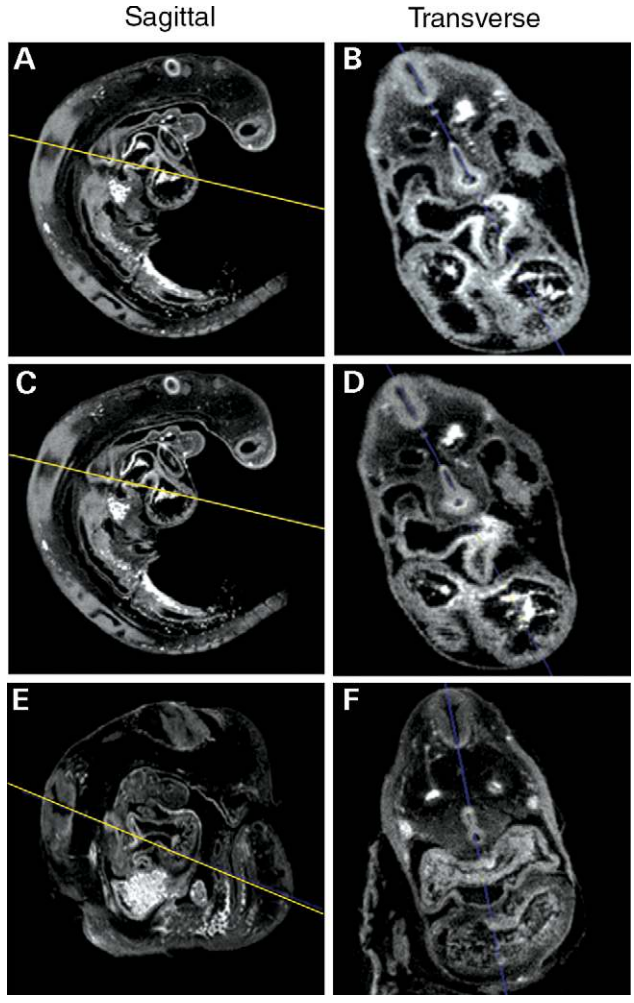

Figure 4. Two-dimensonal digital sections of the point of separation of the foregut. (**A**–**D**) show digital sections of the foregut of the CS12 embryo shown in Fig. 3. (**E**) and (**F**) show digital sections of the foregut of the CS13 embryo shown in Fig. 3. The left hand images in each case show the saggital section of the same embryo. The yellow line depicts the level of the transverse section shown in the right hand side. In each case the transverse was taken perpendicular to the long axis of the foregut at the point indicated by the yellow line. (B) shows the keyhole-shaped lumen of the foregut at CS12 just rostral to the point of fusion in the same embryo shown in (D). Some evidence of lateral septa can be seen with marked thickening of the ventral endoderm. (F) shows the most rostral point of fusion in the CS13 embryo. Note that the shape and position of this point along the rostrocaudal axis of the embryo is very similar to that in the CS12 embryo.

domain in human SRY protein. There are 19 SOX proteins annotated in the human genome that, for reasons of cross-species consistency, are numbered 1–15, 17, 18, 21 and 30. These genes play important and diverse roles in human development as evidenced by the disease-causing mutations found in five *SOX* genes in seven distinct disorders; *SOX2* (3q26.3) in anophthalmos (OMIM 206900), *SOX3* (Xq26.3) in mental retardation with isolated growth hormone deficiency (OMIM 300123) and infundibular hypoplasia and hypopituitarism (OMIM 313430), *SOX9* (17q24) in campomelic dysplasia (OMIM 114290), *SOX10* (22q13) in Waardenburg-Shah syndrome (WSS) (OMIM 277580) and WSS neurological variant (OMIM 609136), and *SOX18* (20q13.3) in hypotrichosis-lymphedema-telangiectasia syndrome (OMIM 607823). Eight SOX protein subgroups, SOXA–SOXH, are defined by the degree of homology outside the HMG domain. SOX2 is a member of the SOXB group with SOX1, SOX3, SOX14 and SOX21. *In vitro* evidence suggests that the C-terminal regions of SOX1–3 act as transcriptional activators, whereas SOX14 and SOX21 contain C-terminal transcriptional repressors. Here, we report robust evidence for a previously undescribed critical role for SOX2 during development of the trachea and oesophagus in humans.

In this study, seven cases of AEG syndrome were screened for mutations in *SOX2*. Five cases had bilateral eye involvement. Four of these had severe bilateral eye

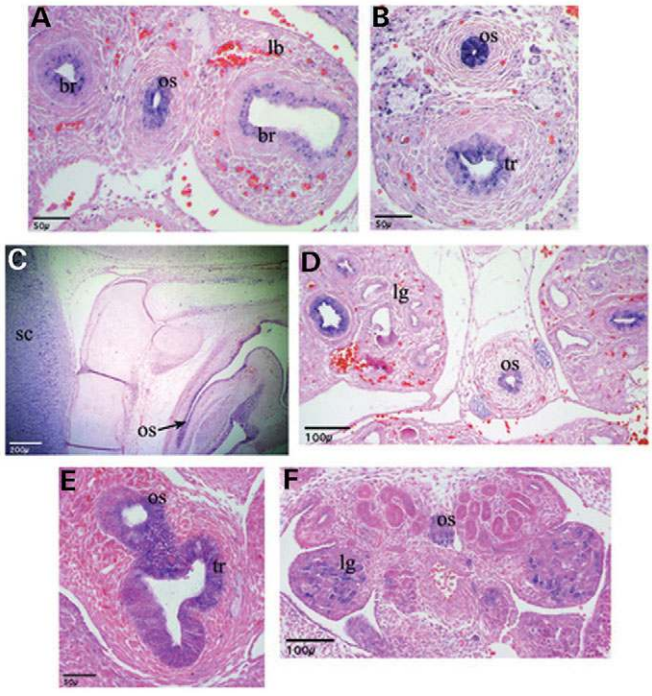

Figure 5. Immunohistochemical analysis of Sox2 in normal and abnormal mouse foregut development. (**A**) and (**B**) show Sox2 immunostaining in transverse sections from 11.5 GD mouse embryos. Strong staining is seen in the oesophagus (os) and trachea (tr) with weaker patchy staining in the main bronchi (br). The lung bud proper (lb) is negative for Sox2. (**C**) shows a saggital section from a 14.5 GD mouse embryo with Sox2 staining visible throughout the foregut endoderm. (**D**) shows a transverse section through a 14.5 GD mouse embryo demonstrating that Sox2 staining is maintained in the oesophagus (os) and the main bronchi within the lung (lg). (**E** and **F**) are transverse sections through *Shh*−/− mouse embryos at 12.5 GD. (E) shows Sox2 staining within the endoderm of a malformed trachea and oesophagus that have failed to fully divide. This type of malformation is well-described in *Shh*−/− mice and is analogous to a tracheo-oesophageal fistula in humans. (F) shows an atretic oesophagus that is Sox2 positive and unusual staining within the lung for Sox2.

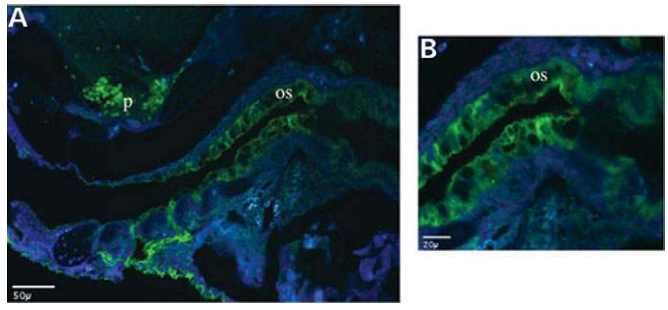

Figure 6. Sox2 expression in the foregut is highly evolutionarily conserved. (**A**) shows immunofluorescent staining in the oesophageal (os) endoderm of a saggital section through a 5-day-old zebrafish embryo. (**B**) shows a higher resolution image of the same section demonstrating that the staining in predominantly cytoplasmic at this stage. The significance of this subcellular distribution is not known but has been observed in several other tissues and cell types (Ann Hever, unpublished data).

malformations; either anophthalmia or extreme microphthalmia. Three of these four were found to carry a *de novo*, apparent loss-of-function mutation in *SOX2*. The remaining bilaterally affected case has unilateral microphthalmia with contralateral coloboma. No mutation was identified in this case, which is compatible with our previous data that suggest optic fissure closure defect is an infrequent finding with *SOX2* mutations (19). The two remaining cases had unilateral anophthalmia or microphthalmia and no *SOX2* mutation was identified in these cases. This again would be compatible with our previous findings that *SOX2* mutations almost always result in severe bilateral eye malformations.

No obvious clinical differences could be identified between the three severely affected cases with an identified *SOX2* mutation and Case 4. FISH and Southern blot analysis could not identify a deletion in or around *SOX2* in this latter case. In addition, detailed point mutation analysis of the entire 5′ and 3′ untranslated regions of *SOX2*, and of the N4 upstream enhancer element, did not reveal any changes. The three *SOX2* mutations in AEG syndrome are remarkably similar in type to that previously reported in the *SOX2* Anophthalmia syndrome (16,17,19): one whole gene deletion, one nonsense mutation and one non-conservative missense mutation in a evolutionarily conserved DNA-binding domain that is critical for protein function.

Case 1 was found to have a whole gene microdeletion associated with a cryptic t(3;7). Interestingly, the telomeric deletion breakpoint, defined by overlapping BAC clones RP11-416O18 and RP11-431C22, appears identical to the telomeric deletion breakpoint associated with the t(3;11) case described by Fantes *et al*. (16). The centromeric breakpoints in these cases differ by 2.1 Mb and we could identify no obvious LCRs in this region that may have mediated the deletion. In addition to *SOX2*, seven other annotated genes, *GNB4*, *ACTL6A*, *NDUFB5*, *USP13*, *PEX5L*, *TTC14* and *FXR1*, were deleted in this case. Given the similarity in features between this case and the cases with intragenic *SOX2* mutations it seems unlikely that any of these seven other genes are having a major haploinsufficent effect. The R74P mutation in Case 3 is similar to the one other reported missense mutation in *SOX2*: this also involves conversion of an invariant residue of the HMG domain, L97, to a helix breaking proline (19). The R74P mutation abolished *Sox2*-dependent transcriptional co-activation of the delta crystallin DC5 enhancer with WT *Pax6* in a yeast one-hybrid assay and is very likely to be causative in this child.

Gene expression and tissue recombination studies in chick and rodent embryos have given us a better understanding of the early molecular and cellular events resulting in dorsoventral separation of the foregut into oesophagus and trachea. The pre-gut endoderm is regionally specified along the anteroposterior (AP) axis of the future foregut [for review see (31,32)]. Sox2 and Pax9 are early markers of the anterior endoderm of the gut tube anterior to the region that is fated to become the duodenum (31,33). Hoxa3 and Hoxb4 are expressed in a similar region in both endoderm and the surrounding mesoderm, whereas Bapx1 is specific to the mesoderm (31). The endoderm is also patterned in the dorsoventral axis and the first morphological evidence of separation of the trachea and oesophagus is the formation of the lung buds in a bilateral symmetrical pattern on the ventral aspect of anterior foregut at 9.5 GD in mouse embryos (34).

The trachea forms only after significant ventral growth of the lung buds (32). Bilateral ridges have been demonstrated on the lateral walls of the foregut dorsal to the lung buds which fuse or merge to create an ascending tracheo-oesophageal septum which separates the dorsal oesophageal tube and the ventral trachea (35). The constriction in the 'figure of eight' shape that we observed in the CS12 human embryos (Fig. 4E,F) may represent the most anterior point of this septum. Interestingly, we could identify no evidence of lateral ridges or septa in an early CS12 human embryos with no evidence of lung bud formation (data not shown). This suggests that the ascending septum may be a very short-lived phenomenon in humans.

In chick embryos, induction of the lung bud is preceeded by, and dependent on Tbx4 expression in the ventral mesenchyme. Tbx4 induces Fgf10 to signal (36) to the underlying forgut endoderm via Fgfr2 isoform IIIb. This signal induces expression of the transcription factor, Titf1 (Nkx2.1). The target genes regulated by Titf1 in the endoderm are not yet known. Targeted inactivation in mouse embryos has provided useful information about the non-redundant roles of these genes during forgut development. *Fgf10*−/− (37) and *FGFR2*−/− (38,39) mice have normal formation of the trachea but failure of distal branching morphogenesis. In contrast, homozygous inactivation of either Titf1(40), retinoic acid (41) or Shh (42,43) signalling in mouse embryos results in no separation of the trachea and oesophagus and almost complete failure of lung bud formation.

Our data suggests that a dosage reduction of SOX2 in the endoderm can result in the failure of normal tracheo-oesophageal separation. However, unlike the mouse models mentioned earlier, we have no evidence that branching morphogenesis in the lung is affected in humans. We have also shown that Sox2 expression is maintained in the forgut of *Shh*−/− mouse embryos. Taken together this suggests that Sox2 is in a different pathway from RARs, Shh, FGF10 and Titf1. In an excellent descriptive study in chick embryos, Ishii *et al*. (29) noted widespread SOX2 expression in the foregut endoderm with regionally specific downregulation where eventration events were signalled by the underlying mesoderm (29). They proposed a model in which SOX2 maintains endoderm in a pluripotent state and must be downregulated prior to any organ-specific differentiation. Thus heterozygous loss of SOX2 may alter the number of cells that are available and competent to participate in lung bud formation as a result of premature differentiation. Further work in animal models will be required before a plausible mechanism for the observed tracheo-oesophageal malformations in AEG syndrome cases can be formulated. *MYNC* and *CDH7* have recently been identified as the causative genes in Feingold (44) and CHARGE (45) syndrome, respectively [for review see; (46)]. Both these disorders have tracheo-oesophageal fistula as a prominent feature and these genes are thus implicated in foregut separation. There is no known link between *SOX2* and either of these genes but identifying any direct or indirect interactions will be important future work.

Similar heterozygous loss-of-function mutations in *SOX2* can cause both SOX2 Anophthalmia syndrome and AEG syndrome. The eye and genital phenotypes in both conditions appear indistinguishable. The foregut malformations in AEG syndrome may thus result from the complement of genetic modifiers (such as *GLI2*, *GLI3* or *SHH*) or through environmental modifiers and/or a stochastic mechanism. With regard to the latter possibility, differences in *SOX2* expression from a WT allele as a result of *cis* polymorphisms may reveal minor differences in dosage sensitivity between the developing foregut and eye. Further studies are required to determine whether tracheo-oesophageal malformations may occur in the absence of ocular defects as a result of *SOX2* mutation.

Morini *et al*. (10). discuss a classification system for AEG syndrome based on a unilateral or bilateral eye phenotype. Here, we have shown that *SOX2* mutations were identified exclusively in bilaterally affected cases. Another notable feature of the molecular analysis is that none of the mutation positive cases had vertebral defects, whereas two mutation negative cases had hemivertebrae and both of these had unilateral eye abnormalities (Table 1). This may define a separate VATER-like subgroup of AEG syndrome. VATER association (OMIM 192350) comprises vertebral defects, anal atresia, tracheo-oesophageal fistula with oesophageal atresia, and radial and renal dysplasia (47). Two of the cases reported by Bardakjian *et al*. (13) are of particular interest as the phenotypes span these proposed classifications, each having bilateral anophthalmia, oesophageal atresia, tracheo-oesophageal fistula, urogenital anomalies and vertabral defects.

The *SOX2* mutations reported here are the first to be identified in AEG syndrome and expand the phenotypes known to be associated with disruption of this gene. *SOX2* deletion in AEG syndrome was not found by Bonneau *et al*. (15). The presence of intragenic mutations was not determined. However, the phenotype of this case, unilateral microphthalmia, oesophageal atresia and fusion of ribs (Table 1), suggests a VATER-like case and therefore unlikely to carry a *SOX2* mutation. The only other gene reported as a candidate for AEG syndrome is *SIX3*, which was screened for mutations in a single case with no mutations detected (8). Interestingly this case, a female with bilateral anophthalmia, is not VATER-like and may therefore be more likely to carry a *SOX2* mutation. Also some cases diagnosed as CHARGE association may in fact be variant AEG syndrome, for example female monozygotic twins with microphthalmia and retinal or optic disc coloboma (one twin affected bilaterally), oesophageal atresia, tracheo-oesophageal fistula, growth and developmental delay, patent ductus arteriosis, chronic otitis media and with no genitourinary anomalies noted (48). Indeed, Case 1 with *SOX2* deletion, was originally considered as severe CHARGE syndrome (1). A full assessment for the presence of *SOX2* mutations is recommended for all forms of AEG syndrome.

MATERIALS AND METHODS

Cases

Seven cases of AEG syndrome were investigated for *SOX2* mutations. The clinical features of six of them have been previously reported (1,2,9,12–14) and the phenotypes of these cases are summarized in Table 1.

Table 1. Phenotypes and *SOX2* mutations in AEG syndrome

Case	Sex	Right eye	Left eye	Oesophagus	Urogenital	Vertebrae	*SOX2* mutation	Reference
1	F[a]	anoph	anoph	atresia, TEF	N[a]			(3)
	M	anoph	anoph	atresia	Hypoplastic kidney			(4)
	M	anoph	anoph	atresia, TEF	Hypospadias	N	del	(1)
	M	anoph	anoph	atresia, TEF	Cryptorchidism	N		(5)
	M	anoph	anoph	atresia, TEF	Micropenis, cryptorchidism	N		(6)
4	F	anoph	anoph	atresia	N			(6)
	M	microph	microph	atresia, TEF	Micropenis, cryptorchidism	N	wt	(2)
2	F	anoph	anoph	atresia	N			(8)
	M	anoph	anoph	atresia, TEF	Renal duplex	N	Q55X	(9)
	F	anoph	anoph	Atresia	N	N		(10)
	M	anoph	anoph	Atresia, TEF	Cryptorchidism			(13)
3	F	microph	microph	Atresia, TEF	N	N	R74P	Current study
	M	anoph	anoph	Atresia, TEF	Hypospadias	Underdeveloped		(13)
	M	anoph	anoph	Atresia, TEF	Cryptorchidism	Hemivertebrae, 11 ribs on left, T3–T8 anomalies		(13)
	M	N	anoph	Atresia, TEF	N	Hemivertebra, 11 ribs on left		(11)
	F	microph	N	Atresia	N[b]	Fusion of 4th/5th left ribs and 1st/2nd right ribs	not del[c]	(15)
5	F	anoph	N	Atresia, TEF	N	Hemivertebra, butterfly vertebra, T1 and S3/S5 anomalies	wt	(12)
6	F	microph	N	Atresia, TEF	N	Hemivertibrae, 13 ribs	wt	(13)
7	M	N	microph	Atresia, TEF	Hypospadias			(7)
	M	CRD	microph, CRD	Atresia, TEF	N	N		(11)
	M	coloboma[d]	microph	Atresia, TEF	N		wt	(14)

The data are arranged in four sections depending on phenotype: section one details cases with bilateral eye and no vertebral defects; section two details cases with bilateral eye and vertebral defects; section three details cases with unilateral eye and vertebral defects; section four details cases with unilateral or distinct bilateral eye and no vertebral defects. TEF, tracheo-oesophageal fistula; N, normal; del, whole gene deletion; wt, wild-type for point mutations; CRD, chorioretinal dysplasia.

[a]28 mm crown-rump length embryo, urogenital system not fully developed.

[b]Normal kidneys and has had a successful pregnancy.

[c]Whole gene deletion not found to be present by Bonneau *et al*. (15).

[d]Iris–choriod–retinal coloboma.

Case 3, who has not been previously reported, is female and the second child of healthy non-consanguineous Caucasian parents. Her elder brother is well but had uncomplicated post-axial polydactyly with a single rudimentary extra digit that was easily removed. A maternal first cousin had cystic fibrosis. She was born at 38 weeks of gestation by emergency caesarian section owing to failed induction following a pregnancy complicated by pre-eclampsia and polyhydramnios. Her birth weight was 2800 g, she was hypotonic, with Apgar scores of 4^1 and 6^5 and required resuscitation with bag and mask ventilation. Extreme bilateral microphthalmia was noted with severe blepharophimosis with ~3 mm palpebral fissure in both eyes. Cranial CT scan showed rudimentary optic globes and chiasm, no evidence of optic nerve within the globe and the ethmoid bone was absent. There was no evidence of hydrocephalus or any other focal abnormality. Shortly after birth, oesophageal atresia and distal tracheo-oesophageal fistula was suspected and radiologically confirmed. Surgical repair of the fistula was carried out on Day 2. No other dysmorphic features were apparent. Chromosome analysis showed an apparently normal female karyotype, 46,XX. On review at 20 months her height was <2nd centile, her weight was on 2–9th centile and head circumference was on the 2nd centile. Gross motor and fine motor development was slightly delayed, thought to be because of her visual problems. There were no concerns about her hearing, speech or social behaviour.

Mutation analysis

Chromosome preparations from lymphoblastoid cell lines were used for FISH analysis of Case 1 and his parents. Clones were obtained from the RP11 human genomic BAC library from BACPAC Resources Center, Oakland, CA, USA and from the Wellcome Trust Sanger Institute. DNA was prepared by a standard mini-prep method and labelled with digoxigenin-11-dUTP or biotin-16-dUTP (Roche) by nick translation. Probe labelling, DNA hybridization and antibody detection were carried out using methods described previously (49). At least 10 metaphases were analysed for each hybridization using a Zeiss Axioskop 2 microscope with the appropriate filters (#83000 for DAPI, FITC and rhodamine; Chroma Technology). Images were collected and merged using a Coolsnap HQ CCD camera (Photometrics) and Smart-Capture 2 (Digital Scientific) software.

The entire coding sequence of *SOX2* was PCR-amplified as two overlapping fragments, the 5′ and 3′ fragments, essentially as described by Fantes *et al*. (16), and the entire untranslated sequence was PCR amplified as four fragments, 5′-UTR and overlapping fragments 3′-UTR.1, 3′-UTR.2 and 3′-UTR.3, essentially as described (50). PCR products were subjected to heteroduplex analysis by DHPLC using a WAVE system 3500, with running conditions established by Navigator 1.5.4 and 1.6.0 software (Transgenomic Inc.). Sequencing template was generated by independent PCR amplification for a second

time and sequenced using BigDye Terminator v3.0 Cycle Sequencing Kit and the ABI 3100 system (Applied Biosystems). Full details of the PCR, DHPLC and sequencing protocols are available in Supplementary Material.

Human embryo analysis

Normal human embryos at Carnegie Stage 12 and 13 were collected with appropriate ethical approval and written consent following chemically induced termination of pregnancy for non-medical reasons. The embryos were non-destructively imaged using OPT (51) and then were returned to the clinical unit for appropriate disposal. The foregut and eye domains within the 3D digital reconstructions of the embryos were defined in individual two-dimensional digital sections using the custom software tool MAPaint (http://genex.hgu.mrc.ac.uk/Software/paint/paint/paint.html).

Immunohistochemistry

WT mouse embryos were harvested from timed matings and fixed overnight in 4% paraformaldehyde at 4°C. *Shh*-null embryos at E12.5, a gift from Laura Lettice, MRC HGU, Edinburgh, UK, were also fixed overnight in 4% paraformaldehyde at 4°C. WT and mutant embryos were dehydrated through a graded ethanol series to 70%, embedded in paraffin wax and cut into 6 μm serial sections. The sections were dewaxed in xylene and rehydrated through a graded ethanol series. Epitope sites were unmasked by boiling in 10 mM citrate buffer pH 6.0 for 1 min. After cooling for 20 min at room temperature (RT), sections were washed several times in PBS and rinsed in dH_2O. All subsequent steps were performed in a humidity chamber. Non-specific binding was reduced by blocking in 10% heat-inactivated sheep serum (Sigma) in PBS for 1 h at RT. Primary antibody, rabbit anti-Sox2 (Chemicon) was diluted to 1:500 in blocking buffer and applied to the sections overnight at 4°C. The sections were washed twice in PBS and once in PBS containing 0.1% Tween-20 for 5 min. Biotinylated anti-rabbit IgG (Vector Laboratories) was diluted 1:500 in blocking buffer and applied to all sections for 1 h at RT. The sections were washed as previously described and then incubated in alkaline phosphatase-conjugated streptavidin (Vector Laboratories) for 1 h at RT. Staining was visualized with BCIP/NBT (Vector Laboratories) containing levamisole to reduce endogenous alkaline phosphatase. After rinsing in PBS, sections were counterstained in eosin and mounted in Histomount (Raymond A. Lamb Ltd).

WT 5-day-old zebrafish embryos were a kind gift from Patricia Yeyati, MRC HGU, Edinburgh, UK. The embryos were fixed and embedded in paraffin wax as above and then cut into 4 μm serial sections. Sections were boiled in 10 mM citrate buffer as above and blocked in 2% heat-inactivated sheep serum, 1% BSA, 0.1% Triton-X-100, 0.05% Tween-20 in PBS for 1 h at RT. Rabbit anti-Sox2 (Chemicon) was diluted in 2% BSA and applied to sections overnight at 4°C. The sections were washed as above and then incubated in fluorescent secondary antibody, Alexa Fluor® 488 (Invitrogen) in 2% BSA for 1 h at RT. Sections were washed extensively and mounted in Vectashield (Vector Laboratories) containing DAPI fluorescent stain at 0.1 μl/ml to visualize cell nuclei.

Yeast one hybrid analysis

Yeast parental strains and protein expression vectors were a kind gift from Yusuke Kamachi, Osaka Univeristy, Osaka, Japan and have been described in detail (52). Briefly, an octamerized sequence of the lens-specific chick DC5 enhancer was placed upstream of the reporter *HIS3* gene and integrated into the genome of the yeast strain YM4271. *Sox2* chick cDNA was cloned into pBD-GAL4 (Cam) (Stratagene) by replacing the GAL4 domain and expressed under the control of the yeast *ADH1* promoter. *Pax6* chick cDNA was cloned adjacent to the GAL4 domain of the expression vector pAD-GAL4 and expressed under the control of the yeast *ADH1* promoter. The Sox2 expression vector carries the *TRP1* gene encoding for tryptophan and the Pax6 vector contains the *LEU2* gene encoding for leucine to allow for selectable growth when transformed into yeast cells. Mutagenesis of *Sox2* chick cDNA was carried out using the QuikChange® Site-Directed Mutagenesis kit (Stratagene). Mutants were identified and confirmed by sequencing in both directions. Reporter yeast cells were co-transformed with Sox2 and Pax6 expression vectors using standard protocols (Clontech Matchmaker One-Hybrid System) and then grown on selectable plates lacking tryptophan, leucine and histidine at 30°C for 5 days.

SUPPLEMENTARY MATERIAL

Supplementary Material is available at HMG Online.

ACKNOWLEDGEMENTS

We thank the families for their support and participation in this research. Z.F. acknowledges the financial support of the project MSM 0021627502. We acknowledge the help of Alison Headford (St Michael's Hospital, Bristol) in retrieving archived specimens from Case 4 and Tanya Bardakjian for help with obtaining samples from Case 6. We thank Francesco Molinaro for help with Case 7.

Conflict of Interest statement. The authors state that they have no conflict of interest.

REFERENCES

1. Curtis Rogers, R. (1988) Unknown cases. Proceedings of the Greenwood Genetic Center. **7**, 57.
2. Shah, D., Jones, R., Porter, H. and Turnpenny, P. (1997) Bilateral microphthalmia, esophageal atresia, and cryptorchidism: the anophthalmia-esophageal-genital syndrome. *Am. J. Med. Genet.*, **70**, 171–173.
3. Schenk, V.W., Geene, M.J., Klein, H.W., Kredeit, P. and Stefanko, S. (1976) A human embryo of 28 mm crown-rump length with cerebral, esophagotracheal and cardiovascular malformations. *Anat. Embryol. (Berl.)*, **150**, 53–62.
4. Sassani, J.W. and Yanoff, (1977) Anophthalmos in an infant with multiple congenital anomalies. *Am. J. Ophthalmol.*, **83**, 43–48.

5. Arroyo, I., Garcia, M.J., Cimadevilla, C.E., Carretero, V., Bermejo, E. and Martinez-Frias, M.L. (1992) Bilateral anophthalmia, esophageal atresia, and right cryptorchidism: a new entity? *Am. J. Med. Genet.*, **43**, 686–687.
6. Sandler, D., Mancuso, A., Becker, T., Zori, R., Hellrung, J., Silverstein, J., Burton, V., Hamosh, A. and Williams, C. (1995) Association of anophthalmia and esophageal atresia. *Am. J. Med. Genet.*, **59**, 484–491.
7. Ulman, I., Herek, O., Genc, A.K. and Erdener, A. (1996) Microphthalmos associated with esophageal atresia. *J. Pediatr. Surg.*, **31**, 433–434.
8. Menetrey, C., Belin, V., Odent, S., de Lumley, L. and Gilbert, B. (2002) Bilateral anophthalmia and oesophageal atresia in a newborn female: a new case of the anophthalmia-oesophageal-genital (AEG) syndrome. *Clin. Dysmorphol.*, **11**, 139–140.
9. Petrackova, I., Pozler, O., Kokstein, Z., Zizka, J., Dedkova, J., Rejtar, P., Fiedler, Z. and Kuliacek, P. (2004) Association of oesophageal atresia, anophthalmia and renal duplex. *Eur. J. Pediatr.*, **163**, 333–334.
10. Morini, F., Pacilli, M. and Spitz, L. (2005) Bilateral anophthalmia and esophageal atresia: report of a new patient and review of the literature. *Am. J. Med. Genet. A*, **132**, 60–62.
11. Imaizumi, K., Ishii, T., Kimura, J., Masuno, M. and Kuroki, Y. (1999) Association of microphthalmia with esophageal atresia: report of two new patients and review of the literature. *Am. J. Med. Genet.*, **87**, 180–182.
12. Hill, C.J., Pilz, D.T., Harper, P.S., Castle, B. and Williams, T.H.C. (2005) Anophthalmia-esophageal-genital syndrome: a further case to define the phenotype. *Am. J. Med. Genet. A*, **132**, 57–59.
13. Bardakjian, T.M. and Schneider, A. (2005) Association of anophthalmia and esophageal atresia: four new cases identified by the anophthalmia/microphthalmia clinical registry. *Am. J. Med. Genet. A*, **132**, 54–56.
14. Messina, M., Ferrucci, E., Buonocore, G., Scarinci, R. and Garzi, A. (2003) Association of microphthalmia and esophageal atresia: description of a patient and review of the literature. *Am. J. Med. Genet. A*, **119**, 184–187.
15. Bonneau, D., Guichet, A., Boussion, F., Lepinard, C., Biquard, F. and Descamps, P. (2004) Absence of deletion at the SOX2 locus in a case of microphthalmia and esophageal atresia. *Am. J. Med. Genet. A*, **131A**, 204.
16. Fantes, J., Ragge, N.K., Lynch, S.A., McGill, N.I., Collin, J.R., Howard-Peebles, P.N., Hayward, C., Vivian, A.J., Williamson, K., van, H.V. and FitzPatrick, D.R. (2003) Mutations in *SOX2* cause anophthalmia. *Nat. Genet.*, **33**, 461–463.
17. Guichet, A., Triau, S., Lepinard, C., Esculapavit, C., Biquard, F., Descamps, P., Encha-Razavi, F. and Bonneau, D. (2004) Prenatal diagnosis of primary anophthalmia with a 3q27 interstitial deletion involving *SOX2*. *Prenat. Diagn.*, **24**, 828–832.
18. Hagstrom, S.A., Pauer, G.J.T., Reid, J., Simpson, E., Crowe, S., Maumenee, I.H. and Traboulsi, E.I. (2005) *SOX2* mutation causes anophthalmia, hearing loss, and brain anomalies. *Am. J. Med. Genet.*: *Part A*, **138A**, 95–98.
19. Ragge, N.K., Lorenz, B., Schneider, A., Bushby, K., de Sanctis, L., de Sanctis, U., Salt, A., Collin, J.R.O., Vivian, A.J., Free, S.L. *et al*. (2005) *SOX2* anophthalmia syndrome. *Am. J. Med. Genet.*: *Part A*, **135A**, 1–7.
20. Zenteno, J.C., Gascon-Guzman, G. and Tovilla-Canales, J.L. (2005) Bilateral anophthalmia and brain malformations caused by a 20-bp deletion in the *SOX2* gene. *Clin. Genet.*, **68**, 564–566.
21. Stevanovic, M., Zuffardi, O., Collignon, J., Lovell-Badge, R. and Goodfellow, P. (1994) The cDNA sequence and chromosomal location of the human *SOX2* gene. *Mamm. Genome*, **5**, 640–642.
22. Kamachi, Y., Uchikawa, M. and Kondoh, H. (2000) Pairing SOX off: with partners in the regulation of embryonic development. *Trends Genet.*, **16**, 182–187.
23. Wilson, M. and Koopman, P. (2002) Matching SOX: partner proteins and co-factors of the SOX family of transcriptional regulators. *Curr. Opin. Genet. Dev.*, **12**, 441–446.
24. Kamachi, Y., Uchikawa, M., Collignon, J., Lovell-Badge, R. and Kondoh, H. (1998) Involvement of Sox1, 2 and 3 in the early and subsequent molecular events of lens induction. *Development*, **125**, 2521–2532.
25. Avilion, A.A., Nicolis, S.K., Pevny, L.H., Perez, L., Vivian, N. and Lovell-Badge, R. (2003) Multipotent cell lineages in early mouse development depend on *SOX2* function. *Genes Dev.*, **17**, 126–140.
26. Thisse, B., Pfumio, S., Fürthauer, M., Loppin, B., Heyer, V., Degrave, A., Woehl, R., Lux, A., Steffan, T. and Charbonnier, X.Q. (2001) Expression of the zebrafish genome during embryogenesis, ZFIN on-line publication.
27. Uchikawa, M., Kamachi, Y. and Kondoh, H. (1999) Two distinct subgroups of Group B *Sox* genes for transcriptional activators and repressors: their expression during embryonic organogenesis of the chicken. *Mech. Dev.*, **84**, 103–120.
28. Wood, H.B. and Episkopou, V. (1999) Comparative expression of the mouse *Sox1*, *Sox2* and *Sox3* genes from pre-gastrulation to early somite stages. *Mech. Dev.*, **86**, 197–201.
29. Ishii, Y., Rex, M., Scotting, P.J. and Yasugi, S. (1998) Region-specific expression of chicken *Sox2* in the developing gut and lung epithelium: regulation by epithelial–mesenchymal interactions. *Dev. Dyn.*, **213**, 464–475.
30. Ferri, A.L., Cavallaro, M., Braida, D., Di Cristofano, A., Canta, A., Vezzani, A., Ottolenghi, S., Pandolfi, P.P., Sala, M., DeBiasi, S. and Nicolis, S.K. (2004) *Sox2* deficiency causes neurodegeneration and impaired neurogenesis in the adult mouse brain. *Development*, **131**, 3805–3819.
31. Grapin-Botton, A. (2005) Antero-posterior patterning of the vertebrate digestive tract: 40 years after Nicole Le Douarin's PhD thesis. *Int. J. Dev. Biol.*, **49**, 335–347.
32. Cardoso, W.V. (2000) Lung morphogenesis revisited: old facts, current ideas. *Dev. Dyn.*, **219**, 121–130.
33. Matsushita, S., Ishii, Y., Scotting, P.J., Kuroiwa, A. and Yasugi, S. (2002) Pre-gut endoderm of chick embryos is regionalized by 1.5 days of development. *Dev. Dyn.*, **223**, 33–47.
34. Spooner, B.S. and Wessells, N.K. (1970) Mammalian lung development: interactions in primordium formation and bronchial morphogenesis. *J. Exp. Zool.*, **175**, 445–454.
35. Williams, A.K., Quan, Q.B. and Beasley, S.W. (2003) Three-dimensional imaging clarifies the process of tracheoesophageal separation in the rat. *J. Pediatr. Surg.*, **38**, 173–177.
36. Sakiyama, J., Yamagishi, A. and Kuroiwa, A. (2003) Tbx4-Fgf10 system controls lung bud formation during chicken embryonic development. *Development*, **130**, 1225–1234.
37. Sekine, K., Ohuchi, H., Fujiwara, M., Yamasaki, M., Yoshizawa, T., Sato, T., Yagishita, N., Matsui, D., Koga, Y., Itoh, N. and Kato, S. (1999) Fgf10 is essential for limb and lung formation. *Nat. Genet.*, **21**, 138–141.
38. Arman, E., Haffner-Krausz, R., Gorivodsky, M. and Lonai, P. (1999) Fgfr2 is required for limb outgrowth and lung-branching morphogenesis. *Proc. Natl Acad. Sci. USA*, **96**, 11895–11899.
39. De Moerlooze, L., Spencer-Dene, B., Revest, J., Hajihosseini, M., Rosewell, I. and Dickson, C. (2000) An important role for the IIIb isoform of fibroblast growth factor receptor 2 (FGFR2) in mesenchymal-epithelial signalling during mouse organogenesis. *Development*, **127**, 483–492.
40. Minoo, P., Su, G.S., Drum, H., Bringas, P. and Kimura, S. (1999) Defects in tracheoesophageal and lung morphogenesis in Nkx2.1(−/−) mouse embryos. *Dev. Biol.*, **209**, 60–71.
41. Mendelsohn, C., Lohnes, D., Decimo, D., Lufkin, T., LeMeur, M., Chambon, P. and Mark, M. (1994) Function of the retinoic acid receptors (RARs) during development (II). Multiple abnormalities at various stages of organogenesis in RAR double mutants. *Development*, **120**, 2749–2771.
42. Litingtung, Y., Lei, L., Westphal, H. and Chiang, C. (1998) Sonic hedgehog is essential to foregut development. *Nat. Genet.*, **20**, 58–61.
43. Motoyama, J., Liu, J., Mo, R., Ding, Q., Post, M. and Hui, C.C. (1998) Essential function of Gli2 and Gli3 in the formation of lung, trachea and oesophagus. *Nat. Genet.*, **20**, 54–57.
44. van Bokhoven, H., Celli, J., van Reeuwijk, J., Rinne, T., Glaudemans, B., van Beusekom, E., Rieu, P., Newbury-Ecob, R.A., Chiang, C. and Brunner, H.G. (2005) MYCN haploinsufficiency is associated with reduced brain size and intestinal atresias in Feingold syndrome. *Nat. Genet.*, **37**, 465–467.
45. Vissers, L.E.L.M., van Ravenswaaij, C.M.A., Admiraal, R., Hurst, J.A., de Vries, B.B.A., Janssen, I.M., van der Vliet, W.A., Huys, E.H.L.P., de Jong, P.J., Hamel, B.C.J. *et al*. (2004) Mutations in a new member of the chromodomain gene family cause CHARGE syndrome. *Nat. Genet.*, **36**, 955–957.
46. Brunner, H.G. and van Bokhoven, H. (2005) Genetic players in esophageal atresia and tracheoesophageal fistula. *Curr. Opin. Genet. Dev.*, **15**, 341–347.
47. Quan, L. and Smith, D.W. (1973) The VATER association. Vertebral defects, Anal atresia, T-E fistula with esophageal atresia, Radial and Renal dysplasia: a spectrum of associated defects. *J. Pediatr.*, **82**, 104–107.

48. Farquhar, J., Carachi, R. and Raine, P.A. (2002) Twins with oesophageal atresia and the CHARGE association. *Eur. J. Pediatr. Surg.*, **12**, 56–58.
49. Chong, S.S., Pack, S.D., Roschke, A.V., Tanigami, A., Carrozzo, R., Smith, A.C.M., Dobyns, W.B. and Ledbetter, D.H. (1997) A revision of the lissencephaly and Miller-Dieker syndrome critical regions in chromosome 17p13.3. *Hum. Mol. Genet.*, **6**, 147–155.
50. Sisodiya, S.M., Ragge, N.K., Cavalleri, G.L., Hever, A., Lorenz, B., Schneider, A., Williamson, K.A., Stevens, J.M., Free, S.L., Thompson, P.J., van Heyningen, V. and Fitzpatrick, D.R. (2006) Role of SOX2 mutations in human hippocampal malformations and epilepsy. *Epilepsia*, **47**, 534–542.
51. Sharpe, J., Ahlgren, U., Perry, P., Hill, B., Ross, A., Hecksher-Sorensen, J., Baldock, R. and Davidson, D. (2002) Optical projection tomography as a tool for 3D microscopy and gene expression studies. *Science*, **296**, 541–545.
52. Kamachi, Y., Uchikawa, M., Tanouchi, A., Sekido, R. and Kondoh, H. (2001) Pax6 and SOX2 form a co-DNA-binding partner complex that regulates initiation of lens development. *Genes Dev.*, **15**, 1272–1286.